

Nuclear moments and isotope shifts of ^{135}La , ^{137}La , and ^{138}La by collinear laser spectroscopy

H. Iimura, M. Koizumi, M. Miyabe, M. Oba, T. Shibata, and N. Shinohara
Japan Atomic Energy Research Institute, Tokai, Ibaraki 319-1195, Japan

Y. Ishida
Institute of Physical and Chemical Research (RIKEN), Wako, Saitama 351-0106, Japan

T. Horiguchi
Hiroshima International University, Kurose-cho, Hiroshima 724-0695, Japan

H. A. Schuessler
Department of Physics, Texas A&M University, College Station, Texas 77843, USA
 (Received 15 August 2003; published 26 November 2003)

The isotope shifts and hyperfine-structure-splitting constants of the $6s^2\ ^1S_0$ - $5d6p\ ^3D_1$ ($\lambda=538.2$ nm) and $5d^2\ ^3P_2$ - $5d6p\ ^1D_2$ ($\lambda=548.4$ nm) transitions of La II have been measured by collinear laser-ion-beam spectroscopy for the accelerator-produced isotopes ^{135}La and ^{137}La , and for the naturally occurring isotopes ^{138}La and ^{139}La . The magnetic moments of the ground states of the isotopes ^{135}La and ^{137}La have been determined to be $\mu(135)=+3.70(9)\mu_N$ and $\mu(137)=+2.700(15)\mu_N$, respectively, and the quadrupole moments to be $Q(135)=-0.4(4)$ e b and $Q(137)=+0.21(3)$ e b. The ratio of the magnetic dipole coupling constants $A(138)/A(139)$ of the level $5d6p\ ^3D_1$ has shown a $-0.35(23)\%$ hyperfine anomaly with respect to the NMR ratio of the nuclear g factors. The change in the mean-square nuclear charge radius determined from the isotope shift between ^{139}La and ^{135}La is $\delta\langle r^2 \rangle^{135,139}=0.08(3)$ fm². This value is smaller than the predictions made by the finite-range droplet model or by the Hartree-Fock plus BCS calculation.

DOI: 10.1103/PhysRevC.68.054328

PACS number(s): 21.10.Ft, 21.10.Ky, 21.60.-n, 27.60.+j

I. INTRODUCTION

The hyperfine structure (HFS) and isotope shift (IS) of atomic spectra can provide information on electromagnetic moments and charge radii. The mass region $A=120$ – 140 has been of particular interest because the analysis of the excitation energies and the transition strengths in Xe ($Z=54$), Ba ($Z=56$), and Cs ($Z=55$) nuclides suggested an increase of quadrupole deformation and a decrease of triaxiality as the neutron number is decreased from $N=82$ to the midshell value of $N=66$ [1,2]. This picture has been supported by measurements of the HFS and IS of Xe [3], Ba [4,5], and Cs [6,7] isotopes. It is interesting whether triaxiality also plays a role in the La ($Z=57$) isotopes and whether the quadrupole deformation behaves similarly. Henry *et al.* [8–10] studied the structure of low-lying levels of the odd-mass La isotopes with $N<82$ by means of β decays, and showed the ability of the weak-coupling model to explain the properties of $^{135}\text{La}_{78}$ and $^{137}\text{La}_{80}$ [8,9]. However, this model fails for $^{133}\text{La}_{76}$, but the particle-plus-triaxial rotor model calculations can account for this nuclide [10].

Lanthanum has two naturally occurring isotopes: the stable $^{139}\text{La}_{82}$, and the extremely long lived isotope $^{138}\text{La}_{81}$ ($T_{1/2}=1.05\times 10^{11}$ yr) which has a low natural abundance of 0.090%. Very few investigations of the HFS and IS have been performed on any isotope other than ^{139}La . The ratios of the HFS constants between ^{137}La and ^{139}La , and the IS between these isotopes, were measured only once by using the method of hollow-cathode interference spectroscopy, the resolution of which was limited by Doppler broadening

[11,12]. In a similar manner the ratios of the HFS constants between ^{138}La and ^{139}La , and the IS between these isotopes, were also measured [12,13]. The IS between ^{138}La and ^{139}La was observed by Childs and Goodman [14] using the laser-rf double-resonance technique. They detected a single HFS peak arising from ^{138}La in each of two transitions, and derived the IS and the ratios of the HFS constants between ^{138}La and ^{139}La . Using resonance-ionization mass spectroscopy Young and Shaw [15] measured the HFS constants of ^{138}La . Benton, Cooke, and Griffith [16] and recently Jin *et al.* [17] utilized atomic-beam laser spectroscopy to obtain the HFS constants and IS for transitions of ^{138}La and ^{139}La .

In this work, collinear laser-ion-beam spectroscopy was performed for the measurements of the HFS constants of ^{139}La , ^{138}La , ^{137}La ($T_{1/2}=6\times 10^4$ yr), and ^{135}La ($T_{1/2}=19.5$ h), as well as the IS between these isotopes. We used a mass-separated ion beam, which is particularly important for the measurement of ^{138}La . In earlier works [14,16] ^{138}La spectra were incomplete because some ^{138}La HFS peaks lay buried under tails of strong ^{139}La peaks, making it impossible to obtain the HFS constants without assuming that the ratios of the HFS constants between ^{138}La and ^{139}La are the same for atomic levels. However, this is only a crude approximation because a large value of hyperfine anomaly is expected [18] due to the very different nuclear spins of ^{139}La ($I^\pi=7/2^+$) and ^{138}La ($I^\pi=5^+$), and in addition the anomaly is not independent of the atomic state [14].

II. EXPERIMENT

The nuclides $^{135,137}\text{La}$ were produced at the JAERI (Japan Atomic Energy Research Institute) tandem accelerator by

TABLE I. Characteristics [22] of the La II optical lines used in this work.

Line (nm)	Lower level			Upper level		
	Configuration	J	Energy (cm^{-1})	Configuration	J	Energy (cm^{-1})
538.2	$6s^2 \ ^1S$	0	7395	$5d6p \ ^3D$	1	25 973
548.4	$5d^2 \ ^3P$	2	6227	$5d6p \ ^1D$	2	24 463
553.7	$5d6s$	2	10 095	$6s6p$	1	28 155

means of the $^{135}\text{Ba}(p, n)$ or $^{137}\text{Ba}(p, 3n)$ reactions for ^{135}La , and the $^{137}\text{Ba}(p, n)$ or $^{138}\text{Ba}(p, 2n)$ reactions for ^{137}La . Pellets of barium carbonate enriched to 93.4% in ^{135}Ba (300 mg/cm^2 thick), 81.9% in ^{137}Ba (400 and 500 mg/cm^2 thick), and 99.7% in ^{138}Ba (400 and 600 mg/cm^2 thick) were bombarded with 200–800 nA proton beams of energy 15, 23, and 29 MeV for the (p, n) , $(p, 2n)$, and $(p, 3n)$ reactions, respectively. The irradiation times were in the 14–28 h range. After bombardment, $^{135,137}\text{La}$ were chemically separated from the target material by an ion exchange method using a minute amount of natural lanthanum as the carrier. The samples of $^{135,137}\text{La}$ were then deposited in the surface ionization ion source of a mass separator [19]. The number of ^{137}La in each sample was estimated to be 10^{14} – 10^{15} atoms by measuring γ rays, and that of ^{135}La to be 10^{13} atoms. In case of the measurements of $^{138,139}\text{La}$, natural samples of lanthanum were used.

The experimental setup is almost the same as our previous ones [20,21]. A single-mode tunable dye laser with a wavemeter (Coherent 699–29) was operated with the dye Rhodamine 110, which was pumped by an Ar-ion laser (Coherent INNOVA-100-20). A part of the laser beam was used for the measurement of the fluorescence spectrum of an I_2 cell, which provides an absolute frequency reference. The relative frequency of the HFS lines was calibrated by a temperature-stabilized confocal Fabry-Perot interferometer with a free spectral range of 150.07(6) MHz (Burleigh CFT-500). The fluorescence photons of the I_2 cell and the transmitted photons through the Fabry-Perot interferometer were detected by photomultiplier tubes (Hamamatsu R374).

A La^+ -ion beam was extracted from the surface ionization ion source, accelerated up to 30 or 40 keV and mass separated by a 55° magnet having a radius of curvature of 1.5 m. The intensity of the beam was typically 50 pA for ^{138}La , 10–100 pA for ^{137}La , and 1 pA for ^{135}La . A counter-propagating laser beam excited the La ions from lower metastable levels to upper levels. The interaction region was defined by a transparent cage kept at the potential of -3 kV, which ensures that the ions were Doppler tuned to resonance only inside the cage. Resonance was observed by detecting the fluorescence light from the upper levels to the levels near the ground state. The fluorescence light was collected by an ellipsoidal mirror onto a cooled photomultiplier tube (Hamamatsu R2256). Color glass filters suppressed stray light from the laser beam. Signals from the photomultiplier tubes were simultaneously counted during the laser frequency scanning, and recorded in a multichannel scaling mode by using a personal-computer based data acquisition system.

The investigated optical transitions are listed in Table I. We measured the hyperfine spectra of the 538.2-nm transition for $^{135,137,138,139}\text{La}$, the 548.4-nm transition for $^{137,138,139}\text{La}$, the 553.7-nm transition for ^{139}La . For each isotope, data were obtained from several scans, typically 8–15 GHz in width and with a 0.75 GHz/min scanning rate. The observed linewidth was 80–150 MHz (full width at half maximum). Typical scans for the 538.2-nm transition of ^{138}La and of ^{137}La are shown in Fig. 1. Because the nuclear spins are 5 and $\frac{7}{2}$ for ^{138}La and ^{137}La , respectively [23], the spectra of these isotopes have three hyperfine components each. Peak assignments were aided by the relative peak intensities predicted by a mathematical model of the system. Assigned F quantum numbers are indicated in Fig. 1 with labeling the lower state (F') first and the upper state (F) second. Peaks not labeled by F quantum numbers are those of ^{139}La , which remained visible next to the $A=137$ or 138 signals even after mass separation due to their strong initial beam intensity. In Fig. 1(c) the summed spectrum for ^{135}La is shown, which was measured over two different ranges. For other transitions, 12 out of 13 ^{139}La peaks, 11 out of 13 ^{138}La peaks, and 10 out of 13 ^{137}La peaks were observed for the 548.4-nm transition; in addition all of nine ^{139}La peaks were recorded for the 553.7-nm transition.

III. RESULTS

The peak centers were determined from a least-squares fit with a Lorentz function and a function describing a tail of the peak. Table II lists the values of magnetic dipole constant A and electric quadrupole constant B obtained by least-squares fitting to the observed peak intervals. Errors are primarily the standard deviation of the distribution of the values from the several scans, but also include propagation of uncertainty of the free spectral range of the Fabry-Perot interferometer. The reference values for ^{139}La [24–26] are from the measurements also using collinear laser-ion-beam spectroscopy. Our values for this isotope are in agreement with those by Höhle, Hühnermann, and Wagner [24], but slightly different from those by Li *et al.* [25].

The relative frequency between one of the hyperfine components of each La isotope and one of the I_2 peaks was obtained by comparison with the Fabry-Perot interferometer spectrum. Using the determined HFS constants, the shifts in the centers of gravity of HFS were deduced. To obtain the IS, the contribution of the Doppler shift was subtracted from the observed shift, and the results are listed in Table III. The uncertainties include the statistical error and the error coming from the accuracy in the measurement of the acceleration

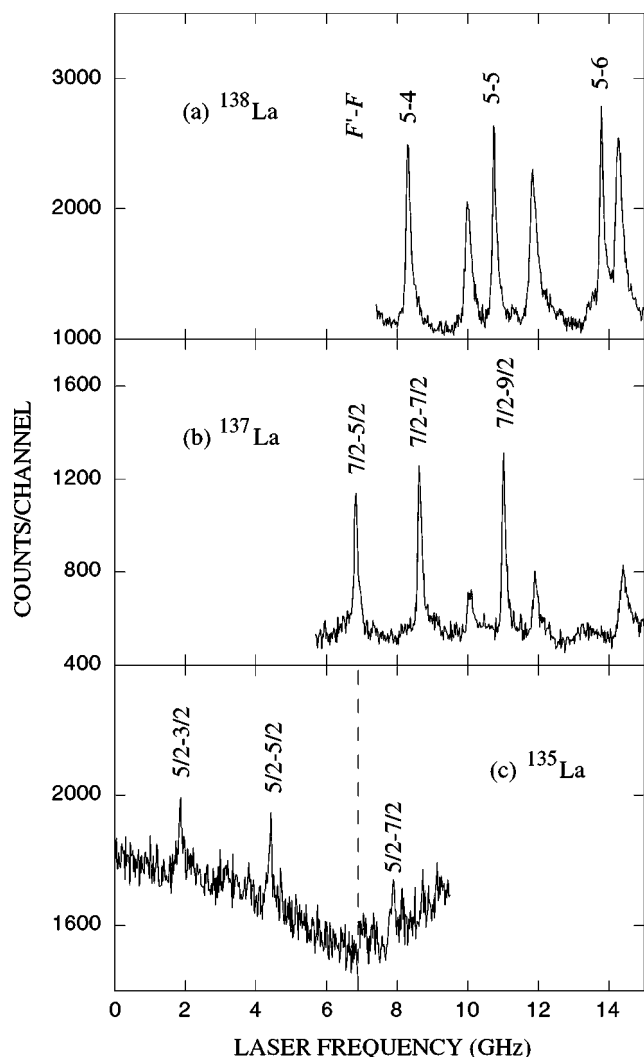


FIG. 1. Typical hyperfine spectra of the 538.2-nm transition of (a) ^{138}La and (b) ^{137}La . The peaks are labeled by the quantum number of the lower state (F') followed by that of the upper state (F). The unlabeled peaks are due to ^{139}La . (c) The lowest recording is a summed spectrum of ^{135}La , which was measured over two different ranges as shown. These spectra are compared at the same beam energy, and the observed shifts in the centers of gravity are due to a combination of their isotope shifts and their different Doppler shifts.

voltage, which was used for the Doppler shift subtraction.

IV. NUCLEAR MOMENTS

A relatively large value of hyperfine anomaly is expected for the odd-even ^{139}La and odd-odd ^{138}La isotopes [18], because of the very different nuclear spins. Fischer *et al.* [13] found $A(138)/A(139)=0.9328(8)$ for the two $5d^26p-5d^26s$ transitions, and interpreted the difference between their result and the NMR ratio of the nuclear g factors as consequence of a hyperfine anomaly. The laser spectroscopy work of Childs and Goodman [14] led them to produce the value of $A(138)/A(139)=0.930\,74(3)$, which is clearly different from the ratio of the g factors of $g(138)/g(139)=0.934\,067\,4(18)$

obtained from NMR measurements by Krüger, Lutz, and Oehler [27]. But the value of Childs and Goodman does not give an actual measurement of the anomaly, since they assumed that the anomalies are the same for the measured $5d6s^2\,^2D_{3/2,5/2}$ states. No other work has reported the existence of a hyperfine anomaly for $^{138,139}\text{La}$. Our present work gives the ratios $A(138)/A(139)=0.9308(22)$ for the $5d6p\,^3D_1$ state, $0.934(3)$ for the $5d6p\,^1D_2$ state, $0.933(6)$ for the $5d^2\,^3P_2$ state. The first one shows a difference from the NMR ratio outside the error, and the hyperfine anomaly, defined as $^{138}\Delta^{139}=[A(138)/A(139)][g(139)/g(138)]-1$, is $-0.35(23)\%$. It is possible that the 3D_1 state contains a substantial admixture of $s_{1/2}$ electron to probe the nuclear volume, because of the complex level structure of La ion. As an additional result, the $B(138)/B(139)$ ratios of $2.1(4)$, $1.3(12)$, and $1.98(20)$ have been obtained in this work for the 3D_1 , 1D_2 , and 3P_2 states, respectively, showing agreement with a NMR ratio of the nuclear electric quadrupole moments of $Q(138)/Q(139)=2.15(17)$ [27].

The magnetic dipole moments of ^{137}La and ^{135}La have been derived from the ^{139}La magnetic dipole moment $\mu(139)=+2.783\,045\,5(9)\mu_N$ [28] and our measured A values for these isotopes. In the case of ^{137}La , the weighted mean of our ratios $A(137)/A(139)$ for the 3D_1 , 1D_2 , and 3P_2 states has been used. The results are listed in Table IV, where the errors arise from the propagation of errors in the A values and also include the uncertainty in the ^{139}La magnetic moment. The hyperfine anomaly is expected to be small for ^{139}La , ^{137}La , and ^{135}La , because these nuclei have similar nucleon configurations. We estimated the upper limit of the hyperfine anomaly to be 0.5%, and the magnetic moments were assigned an additional error due to it. The present value of ^{137}La is in good agreement with that given in Ref. [28], which recalculated the value from Ref. [11] with the reference of ^{139}La . No error due to the hyperfine anomaly is included in the error of this reference value [11]. The electric quadrupole moments of ^{137}La and ^{135}La have been obtained from the ^{139}La electric quadrupole moment $Q(139)=+0.20(1)\,e\,b$ [29] and our ratios of B values for these isotopes, the results of which are listed in Table IV. The uncertainty is due to the errors in the values of B and $Q(139)$. The present result of ^{137}La is slightly smaller than the reference value [28].

In Table IV the nuclear moments of the $\frac{5}{2}^+$ first excited state of ^{133}Cs are also shown. As seen in the table, the nuclear moments of this state are close to those of the $\frac{5}{2}^+$ ground state of ^{135}La , supporting similar configurations for these states. Kisslinger and Sorensen [30] in their calculation based on a pairing-plus-quadrupole model obtained the nuclear moments of the $\frac{7}{2}^+$ and $\frac{5}{2}^+$ states of ^{137}La and ^{133}Cs . For the magnetic moments the values of Kisslinger and Sorensen are smaller than the experimental values, while they show the opposite trend for the quadrupole moments.

V. MEAN-SQUARE NUCLEAR CHARGE RADIUS

The IS $\delta\nu_{\text{IS}}^{AA'}=\nu_{A'}-\nu_A$ is composed of the normal mass shift (NMS), the specific mass shift (SMS), and the field shift (FS):

TABLE II. La II hyperfine structure constants measured in the present experiment in comparison with previous results.

Mass number	I	Level	A (MHz)	B (MHz)
139	$\frac{7}{2}$	$5d^2\ ^3P_2$	-157.3(5)	-51(3)
			-158.1(4) ^a	-45(11) ^a
			-160.1(12) ^b	-37.9(31) ^b
		$5d6s\ J=2$	47.7(6)	38(6)
			48.1(1) ^a	40(2) ^a
			48.5(6) ^c	39.5(42) ^c
			449.6(6)	16(6)
$5d6p\ ^1D_2$	549.1(7)	26(3)		
$5d6p\ ^3D_1$	794.4(11)	-11(3)		
138	5	$5d^2\ ^3P_2$	-146.8(9)	-101(8)
		$5d6p\ ^1D_2$	420.1(13)	20(17)
		$5d6p\ ^3D_1$	511.1(10)	55(9)
137	$\frac{7}{2}$	$5d^2\ ^3P_2$	-151.9(13)	-54(11)
		$5d6p\ ^1D_2$	436.3(21)	16(15)
		$5d6p\ ^3D_1$	532.9(14)	28(5)
135	$\frac{5}{2}$	$5d6p\ ^3D_1$	1023(26)	-50(50)

^aReference [24].

^bReference [25].

^cReference [26].

$$\delta\nu_{iIS}^{AA'} = \delta\nu_{iNMS}^{AA'} + \delta\nu_{iSMS}^{AA'} + \delta\nu_{iFS}^{AA'}$$

The NMS is calculated as $\delta\nu_{iNMS}^{AA'} = \nu_A m (M_{A'} - M_A) / M_A M_{A'}$, where m and M_A are the masses of the electron and an ion with mass number A , respectively. The SMS can theoretically be evaluated only with limited precision. The FS, which is induced by the finite nuclear charge distribution, is written as $\delta\nu_{iFS}^{AA'} = E_i f(Z) \lambda$ [31], where E_i and $f(Z)$ are the electronic factor and the relativistic correction factor, respectively. The nuclear parameter λ gives changes in the mean-square nuclear charge radius (MSCR) and higher-order moments. To estimate the contribution of the SMS to the observed IS, we performed a King-plot analysis, introducing the modified IS $\delta\nu_{i\text{ mod}}$ as

$$\delta\nu_{i\text{ mod}}^{AA'} = (\delta\nu_{iIS}^{AA'} - \delta\nu_{iNMS}^{AA'}) \frac{M_A M_{A'}}{M_{A'} - M_A} \frac{M_{138} - M_{139}}{M_{139} M_{138}}$$

The modified IS's of two transitions i and j are connected by the following linear equation:

TABLE III. Isotope shifts obtained in La II transitions.

Line (nm)	Isotope shifts (MHz)		
	135-139	137-139	138-139
538.2	-240(70)	116(17)	599(10)
548.4		7(23)	-14(20)

$$\delta\nu_{i\text{ mod}}^{AA'} = \frac{E_i}{E_j} \delta\nu_{j\text{ mod}}^{AA'} + \delta\nu_{iSMS}^{139,138} - \frac{E_i}{E_j} \delta\nu_{jSMS}^{139,138}$$

In Fig. 2 our modified IS data are plotted against corresponding ones of the 517.7-nm transition in La I measured by Fischer, Hühnermann, and Mandrek [12]. The slope of the King line E_i/E_j gives the ratio of the electronic factor of the FS, and the intercept corresponds to $\delta\nu_{iSMS}^{139,138} - (E_i/E_j) \delta\nu_{jSMS}^{139,138}$. The ratios of the electronic factors determined from the King plots of Fig. 2 are listed in Table V. The SMS of the 517.7-nm transition can be evaluated to be $\delta\nu_{jSMS} = (0.3 \pm 0.9) \delta\nu_{jNMS}$ [31], because this transition corresponds to the $5d^2 6s-5d^2 6p$ transition. Using this value,

TABLE IV. Magnetic dipole and electric quadrupole moments of the ground states in ¹³⁷La and ¹³⁵La, and those of the first excited state in ¹³³Cs.

Nucleus	Level (keV)	I^π	μ_{expt} (μ_N)	μ_{theor} (μ_N) ^a	Q_{expt} (e b)	Q_{theor} (e b) ^a
¹³⁷ La ₈₀	0	$\frac{7}{2}^+$	+2.700(15) ^b	+2.27	+0.21(3) ^b	+0.38
			+2.695(6) ^c		+0.24(7) ^c	
¹³⁵ La ₇₈	0	$\frac{5}{2}^+$	+3.70(9) ^b		-0.4(4) ^b	
¹³³ Cs ₇₈	81	$\frac{5}{2}^+$	+3.45(2) ^c	+3.03	-0.33(2) ^c	-0.96

^aReference [30].

^bPresent work.

^cReference [28].

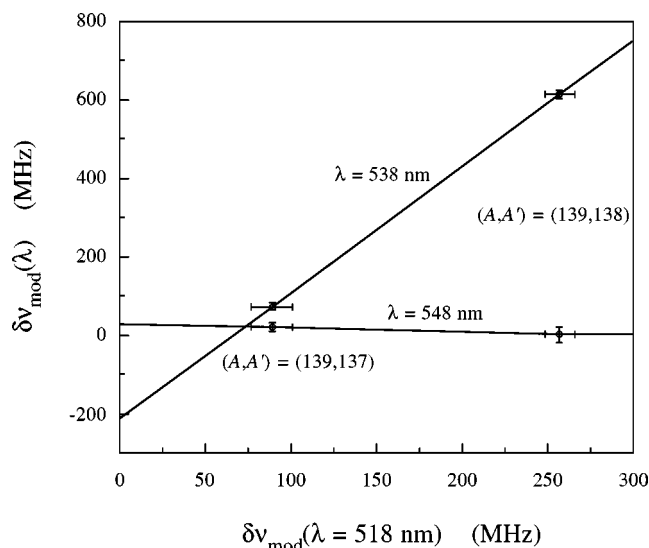


FIG. 2. King plots of the modified isotope shifts in the 538.2- and 548.4-nm lines in La II, referred to the 517.7-nm line in La I.

the SMS of the measured transitions was separated from the IS. Our results of the SMS for the isotope pair ^{138}La - ^{139}La are listed in Table V for the observed 538.2- and 548.4-nm transitions. The errors are due to the errors in the values of IS and also include the uncertainty in the SMS of the 517.7-nm transition. As seen in Table V, the electronic factor of the 538.2-nm transition is 3.2 times larger than that of the 517.7-nm transition. This value is comparable to the experimental value of 2.02(20) [12] for the analog transition in La I, of which the lower level is in a $5d6s^2$ configuration and the upper level is composed of $5d6s6p$ and $5d^26p$ configurations.

After the SMS was estimated, the FS for the isotope pair ^{139}La - ^{135}La was derived to be $\delta v_{\text{FS}}^{135,139} = -770(380)$ MHz from the observed IS. The error comes mainly from the uncertainty in the SMS. By dividing this FS by that of a reference pair ^{138}La - ^{139}La , the relative λ value was obtained to be $\lambda_{\text{rel}}^{135,139} = -0.91(39)$, where we neglected the variation of $f(Z)$ with mass number. Aufmuth, Heilig, and Steudel [31] gave $\lambda^{139,138} = -0.080(10) \text{ fm}^2$ by summing the results of Refs. [12,14]. Using this value, we obtained $\lambda^{135,139}$. For the La isotopes, the moments higher than $\langle r^2 \rangle$ contribute about 4% to λ [32]. Taking this contribution into account, the value of $\delta \langle r^2 \rangle^{135,139}$ was obtained to be

$$\delta \langle r^2 \rangle^{135,139} = 0.08(3) \text{ fm}^2.$$

The corresponding values for the isotonic nuclei are $\delta \langle r^2 \rangle^{134,138} = 0.053(16) \text{ fm}^2$ [4] for Ba, and $\delta \langle r^2 \rangle^{136,140}$

TABLE V. Results of the ratios of the electronic factors $E(\lambda)/E(517.7)$ and the SMS between ^{138}La and ^{139}La . The calculated NMS's are also listed.

Line (nm)	$E(\lambda)/E(517.7)$	NMS (MHz)	SMS (MHz)
538.2	3.2(3)	-16	-230(90)
548.4	-0.10(14)	-16	29(26)

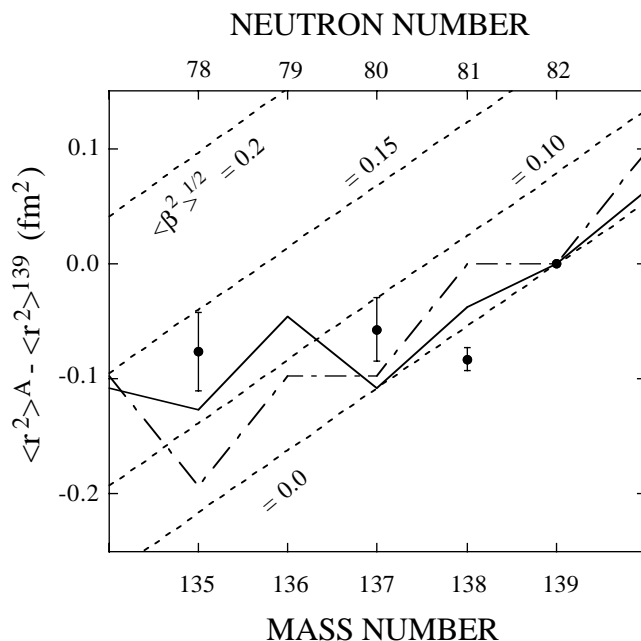


FIG. 3. Experimental changes in the MSCR, $\langle r^2 \rangle^A - \langle r^2 \rangle^{139}$, for the La isotopes (solid circles), where that of $A=135$ is from this work and others are from Ref. [31]. The theoretical predictions of the FRDM (solid line) and HFBCS (dash-dotted line) are also shown for comparison. Droplet-model isodeformation lines are indicated as dotted lines.

$= 0.031(9) \text{ fm}^2$ [21] for Ce, being comparable with the present result of La. Figure 3 shows experimental $\delta \langle r^2 \rangle^{139,A}$, where the value of $A=135$ is the present one and others are from Ref. [31]. Because Aufmuth, Heilig, and Steudel [31] gave λ , a correction of 4% from the higher-order moments is applied to their values in Fig. 3.

For an interpretation of the result, the experimental $\delta \langle r^2 \rangle^{139,A}$ values can be compared to the predictions of the droplet model. Using the droplet model the changes in the MSCR were calculated from

$$\delta \langle r^2 \rangle^{139,A} = \frac{3}{5} \left[R_Z^{2(A)} \left(1 + \frac{5}{4\pi} \langle \beta^2 \rangle^A \right) - R_Z^{2(139)} \left(1 + \frac{5}{4\pi} \langle \beta^2 \rangle^{139} \right) \right],$$

where R_Z is the proton sharp radius [33], and β is the quadrupole deformation parameter. The results are shown by the parallel dotted lines in Fig. 3, where the assumption was made that the singly magic ^{139}La has a deformation of zero. It can be seen that the deformation of the odd-mass La nuclei gently increases when neutrons are removed in pairs from the magic number $N=82$.

Also, Fig. 3 includes the theoretical predictions by the finite-range droplet model (FRDM) [34] and the Hartree-Fock-BCS method (HFBCS) [35]. Those of the FRDM were calculated by us using the deformation parameters given in Ref. [34]. The MSCR's predicted by these models are smaller than the experimental values for the odd mass ^{137}La and especially for ^{135}La . Such a discrepancy was already

observed for the case of Ba, where the density-dependent Hartree-Fock (DDHF) calculation [36] predicted too small MSCR values at $N < 82$. Mueller *et al.* [5] suggested that this discrepancy in Ba can, at least partly, be attributed to the static character of deformation in the DDHF calculation. This suggestion is reasonable because Ba nuclei in this mass region have dynamic triaxial shapes or, in other words, they are γ soft [37]. For La, it can similarly be suggested that the collective zero-point motion in the γ direction influences the MSCR. This picture can, at least partly, explain the discrepancy between the experimental MSCR values and the theoretical predictions, because the FRDM and the HFBCS deal only with static properties.

VI. CONCLUSIONS

The IS and HFS of the 1S_0 - 3D_1 and 3P_2 - 1D_2 transitions of the singly charged ^{135}La , ^{137}La , ^{138}La , and ^{139}La ions have been measured by collinear laser-ion-beam spectroscopy. The ratio of the magnetic dipole coupling constants $A(138)/A(139)$ of the 3D_1 level has shown a hyperfine anomaly with respect to the NMR ratio of the nuclear g factors. The magnetic dipole moments and the electric quadrupole moments of the ground states of ^{135}La and ^{137}La were determined. The nuclear moments of the ground state of

^{135}La were found to be close to those of the first excited state of ^{133}Cs , supporting similar configurations for these states. As for the IS, the contributions of SMS and FS were separated by using a King-plot analysis. From the FS between ^{139}La and ^{135}La , we determined the change in the MSCR $\delta\langle r^2 \rangle^{135,139}$ for the first time. By comparing the result with the droplet-model predictions, it can be seen that the deformation of the odd-mass La nuclei gently increases as the neutron number is decreased from the magic number. It was also found that the experimental $\delta\langle r^2 \rangle^{135,139}$ value is smaller than the FRDM or HFBCS predictions. This fact can, at least partly, be attributed to shape fluctuations. Although this feature has been seen in the present work at four neutrons away from shell closure, it is necessary to examine these models in more detail by comparing with the MSCR values for more neutron-deficient La nuclei. Work to measure them is already in progress by our laser spectroscopy collaboration at the ISAC facility at TRIUMF.

ACKNOWLEDGMENTS

We wish to thank M. Ito for performing the chemistry. We also wish to thank the crew of the JAERI tandem accelerator for generating proton beams.

-
- [1] J. Yan, O. Vogel, P. von Brentano, and A. Gelberg, *Phys. Rev. C* **48**, 1046 (1993).
 - [2] O. Vogel, A. Gelberg, R. V. Jolos, and P. von Brentano, *Nucl. Phys. A* **576**, 109 (1994).
 - [3] W. Borchers, E. Arnold, W. Neu, R. Neugart, K. Wendt, G. Ulm, and ISOLDE Collaboration, *Phys. Lett. B* **216**, 7 (1989).
 - [4] K. Bekk, A. Andl, S. Göring, A. Hanser, G. Nowichi, H. Rebel, and G. Schatz, *Z. Phys. A* **291**, 219 (1979).
 - [5] A. C. Mueller, F. Buchinger, W. Klempt, E. W. Otten, R. Neugart, C. Ekström, J. Heinemeier, and ISOLDE Collaboration, *Nucl. Phys. A* **403**, 234 (1983).
 - [6] C. Thibault, F. Touchard, S. Büttgenbach, R. Klapisch, M. de Saint Simon, H. T. Duong, P. Jacquinet, P. Juncar, S. Liberman, P. Pillet, J. Pinard, J. L. Vialle, A. Pesnelle, ISOLDE Collaboration, and G. Huber, *Nucl. Phys. A* **367**, 1 (1981).
 - [7] A. Coc, C. Thibault, F. Touchard, H. T. Duong, P. Juncar, S. Liberman, J. Pinard, M. Carre, J. Lerme, J. L. Vialle, S. Büttgenbach, A. C. Mueller, A. Pesnelle, and ISOLDE Collaboration, *Nucl. Phys. A* **468**, 1 (1987).
 - [8] E. A. Henry, N. Smith, P. G. Johnson, and R. A. Meyer, *Phys. Rev. C* **12**, 1314 (1975).
 - [9] E. A. Henry and R. A. Meyer, *Phys. Rev. C* **12**, 1321 (1975).
 - [10] E. A. Henry and R. A. Meyer, *Phys. Rev. C* **18**, 1814 (1978).
 - [11] W. Fischer, H. Hühnermann, and K. Mandrek, *Z. Phys.* **254**, 127 (1972).
 - [12] W. Fischer, H. Hühnermann, and K. Mandrek, *Z. Phys.* **269**, 245 (1974).
 - [13] W. Fischer, H. Hühnermann, K. Mandrek, and H. Ihle, *Phys. Lett.* **40B**, 87 (1972).
 - [14] W. J. Childs and L. S. Goodman, *Phys. Rev. A* **20**, 1922 (1979).
 - [15] J. P. Young and R. W. Shaw, *J. Opt. Soc. Am. B* **12**, 1398 (1995).
 - [16] D. M. Benton, J. L. Cooke, and J. A. R. Griffith, *J. Phys. B* **27**, 4365 (1994).
 - [17] W. G. Jin, T. Endo, H. Uematsu, T. Minowa, and H. Katsuragawa, *Phys. Rev. A* **63**, 064501 (2001).
 - [18] Yu. P. Gangrsky, D. V. Karaivanov, K. P. Marinova, B. N. Markov, and S. G. Zemlyanoi, *Z. Phys. D: At., Mol. Clusters* **41**, 251 (1997).
 - [19] S. Ichikawa, T. Sekine, M. Oshima, H. Iimura, and Y. Nakahara, *Nucl. Instrum. Methods Phys. Res. B* **70**, 93 (1992).
 - [20] H. Iimura, Y. Nakahara, S. Ichikawa, M. Kubota, and T. Horiguchi, *Phys. Rev. C* **50**, 661 (1994).
 - [21] Y. Ishida, H. Iimura, S. Ichikawa, and T. Horiguchi, *J. Phys. B* **30**, 2569 (1997).
 - [22] W. C. Martin, R. Zalubas, and L. Hagan, *Atomic Energy Levels: The Rare Earth Elements* (U.S. Government Printing Office, Washington, DC, 1978), NSRDS-NBS 60.
 - [23] R. B. Firestone, V. S. Shirley, C. M. Baglin, S. Y. F. Chu, and J. Zipkin, *Table of Isotopes*, 8th ed. (Wiley, New York, 1996).
 - [24] C. Höhle, H. Hühnermann, and H. Wagner, *Z. Phys. A* **304**, 279 (1982).
 - [25] G. W. Li, X. M. Zhang, F. Q. Lu, X. J. Peng, and F. J. Yang, *Jpn. J. Appl. Phys., Part 1* **40**, 2508 (2001).
 - [26] M. Li, H. Ma, M. Chen, Z. Chen, F. Lu, J. Tang, and F. Yang, *Phys. Scr.* **61**, 449 (2000).
 - [27] H. Krüger, O. Lutz, and H. Oehler, *Phys. Lett.* **62A**, 131

- (1977).
- [28] P. Raghavan, *At. Data Nucl. Data Tables* **42**, 189 (1989).
- [29] J. Bauche, J. F. Wyart, Z. B. Ahmed, and K. Guidara, *Z. Phys. A* **304**, 285 (1982).
- [30] L. S. Kisslinger and R. A. Sorensen, *Rev. Mod. Phys.* **35**, 853 (1963).
- [31] P. Aufmuth, K. Heilig, and A. Steudel, *At. Data Nucl. Data Tables* **37**, 455 (1987).
- [32] G. Torbohm, B. Fricke, and A. Rosén, *Phys. Rev. A* **31**, 2038 (1985).
- [33] W. D. Myers and K. H. Schmidt, *Nucl. Phys.* **A410**, 61 (1983).
- [34] P. Möller, J. R. Nix, W. D. Myers, and W. J. Swiatecki, *At. Data Nucl. Data Tables* **59**, 185 (1995).
- [35] S. Goriely, F. Tondeur, and J. M. Pearson, *At. Data Nucl. Data Tables* **77**, 311 (2001).
- [36] M. Epherre, G. Audi, and X. Campi, in *Proceedings of the Fourth International Conference on Nuclei Far From Stability, Helsingør, 1981* (CERN, Geneva, 1981), p. 62.
- [37] R. F. Casten and P. von Brentano, *Phys. Lett.* **152**, 22 (1985).